# Movement ecology and habitat selection of Asian elephants (*Elephas maximus*) in the Gelephu–Sarpang region, Bhutan


## Abstract

*Human–elephant conflict and habitat fragmentation represent the foremost threats to Asian elephant (Elephas maximus) populations across their 13-state range, yet fine-scale, autocorrelation-aware movement analyses remain scarce for populations in the northern foothill landscapes of South Asia. GPS satellite collars were deployed on four wild Asian elephants in the Gelephu–Sarpang region of south-central Bhutan, yielding 39,578 validated fixes at 10-min intervals over 328–545 days per individual. Because consecutive GPS relocations are temporally autocorrelated, a movement-aware analytical framework was applied: autocorrelated kernel density estimation (AKDE;* ***ctmm*** *v1.3.0) for home-range quantification, integrated step selection functions (iSSF;* ***amt*** *v0.3.1) for habitat selection, and hidden Markov models (HMM;* ***momentuHMM*** *v1.5.8) for behavioural state classification. AKDE 95% home ranges varied 12-fold among individuals (170–2,036 km²), reflecting substantial individual variation in movement tactics. The iSSF revealed strong avoidance of high-elevation terrain (hazard ratio [HR] = 0.26, 95% CI 0.22–0.30, per 1 SD increase in elevation) and cropland (HR = 0.90, 95% CI 0.88–0.93), with positive selection for vegetation greenness (NDVI; HR = 1.15, 95% CI 1.10–1.20). A parallel global resource selection function (RSF) returned no significant covariate effects — an outcome attributable to spatial autocorrelation among used relocations rather than an absence of habitat selection. Three HMM states were resolved: Resting (16–30% of fixes), Foraging (23–40%) and Traveling (37–62%), with pronounced state fidelity in the Traveling state (self-transition probability = 0.68). Inference is restricted to the four tracked individuals; population-level extrapolation is not warranted from this sample. Collectively, these results demonstrate that movement-aware modelling recovers biologically coherent habitat selection signals that conventional IID-based frameworks obscure, and provide a reproducible analytical blueprint applicable to elephant range states across South and South-East Asia.*



**Keywords:** Asian elephant; *Elephas maximus*; movement ecology; autocorrelated kernel density estimation; step selection function; hidden Markov model; ctmm; human–elephant conflict; Bhutan; GPS telemetry

## 1. Introduction

The Asian elephant (*Elephas maximus*) is classified as Endangered on the IUCN Red List, with an estimated 40,000–52,000 individuals persisting across 13 range states (Williams et al., 2020). Habitat fragmentation and human–elephant conflict (HEC) — encompassing crop depredation, property damage and human casualties — represent the principal threats to long-term population viability throughout the species' range (Sukumar, 2006; Leimgruber et al., 2003). Evidence-based conservation planning demands accurate characterisation of how elephants partition space and select habitat across ecologically relevant temporal scales (Nathan et al., 2008).

High-frequency GPS satellite telemetry has transformed the capacity to document elephant movement at fine temporal resolution, but the statistical treatment of such data has not always kept pace with the methodology of data collection. Consecutive GPS relocations are temporally autocorrelated — the position of a moving animal at time $t$ is non-independent of its position at time $t - \Delta t$ — and this autocorrelation violates the independent and identically distributed (IID) assumption underpinning conventional home-range estimators (minimum convex polygons [MCP] and kernel density estimation [KDE]) and global resource selection functions (RSF) (Fleming et al., 2015; Noonan et al., 2019). When the IID assumption is violated, MCP and KDE positively bias home-range area estimates, and global RSF conflates movement constraints with habitat preference, producing systematically attenuated or null covariate effects that can mislead region planning and protected area designation (Fleming et al., 2015; Avgar et al., 2016). Movement-aware inference is therefore not a methodological refinement but a scientific prerequisite for habitat selection analysis of high-frequency GPS telemetry data.

Continuous-time movement models implemented in the **ctmm** R package correct for autocorrelation structure and produce statistically rigorous AKDE home-range estimates with proper confidence intervals (Calabrese et al., 2016; Noonan et al., 2019). Integrated step selection functions (iSSF) condition habitat availability sampling on the empirically observed step-length and turning-angle distributions, explicitly coupling the movement process with habitat selection and eliminating the pseudo-replication inherent in global RSF (Thurfjell et al., 2014; Avgar et al., 2016; Signer et al., 2019). Hidden Markov models (HMM) enable objective, data-driven classification of movement-based behavioural states without requiring contemporaneous behavioural observation (Langrock et al., 2012; McClintock & Michelot, 2020).

Despite these methodological advances, the complete modern toolkit — ctmm AKDE, amt iSSF and momentuHMM applied simultaneously to the same telemetry dataset — has not previously been demonstrated for Asian elephants in the northern foothill landscapes of Bhutan. The Gelephu–Sarpang region of south-central Bhutan, a mosaic of tropical forest, riverine grassland, agriculture and human settlements, forms part of a transboundary landscape connecting Bhutan with the Manas National Park complex in Assam, India, and constitutes a critical but analytically understudied elephant habitat. Beyond its regional significance, the region provides an appropriate case study for demonstrating movement-aware analytical approaches applicable across the full range of *Elephas maximus*.

The objectives of this study were to: (1) estimate home-range areas using ctmm AKDE and compare them with conventional KDE and MCP estimators to quantify the practical consequences of autocorrelation correction; (2) quantify habitat selection using both a global

RSF and an iSSF to illustrate the necessity of movement-aware modelling; (3) classify movement-based behavioural states (Resting, Foraging, Traveling) using a 3-state HMM; and (4) derive conservation implications for region management and HEC mitigation in south-central Bhutan and the broader South Asian elephant landscape.

## 2. Methods

### 2.1 Study area

The study area encompasses the Gelephu–Sarpang and adjoining Indian plains (26.44–27.07°N, 89.75–91.15°E). Elevation ranges from approximately 150 m to over 2,000 m above sea level, creating a steep tropical-to-montane gradient within a geographically compact landscape. Dominant land cover types include sal (*Shorea robusta*) forest, riverine grasslands, paddy and maize cultivation, and expanding peri-urban settlements. Mean annual rainfall exceeds 2,000 mm, delivered primarily during the June–September monsoon. The region is contiguous with the transboundary Manas National Park complex in Assam, India.

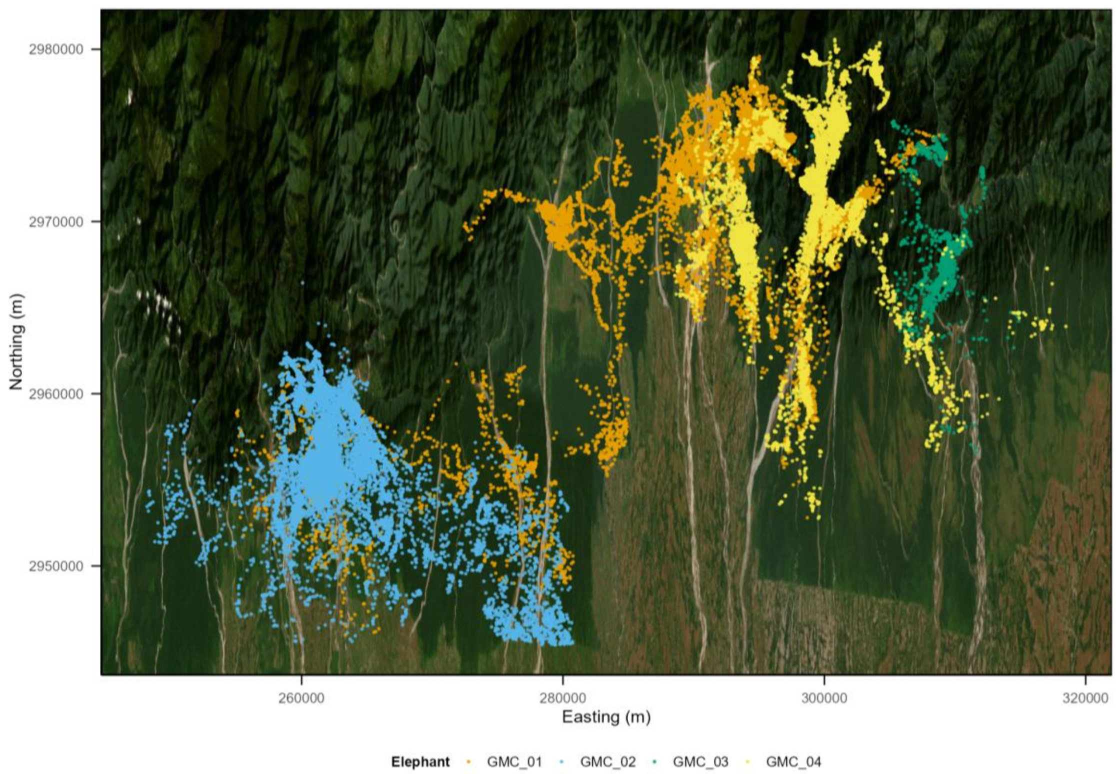


***Figure 1.*** *Study area map of the Gelephu–Sarpang region, south-central Bhutan (26.44–27.07°N, 89.75–91.15°E). Basemap shows elevation (m a.s.l.) with major rivers, road network and protected area boundaries. GPS collar deployment sites are indicated.*

### 2.2 GPS collar deployment and data preparation

Four wild Asian elephants (*designated as GMC_01 to GMC_04*) were equipped with GPS satellite collars by the Department of Forests and Park Services, Royal Government of Bhutan, following standard immobilisation protocols. Collars recorded relocations at 10-min intervals. Tracking durations were: *GMC_01*, 545 days (3 October 2024 – 1 April 2026); GMC_02, 541 days (7 October 2024 – 1 April 2026); GMC_03, 328 days (24 December 2024 – 17 November

2025); GMC_04, 444 days (13 January 2025 – 1 April 2026). All timestamps were converted to Asia/Thimphu time (UTC+6).

Quality control was applied in sequential steps using a validated R pipeline (functions_qc.R; available in the project repository): (i) removal of relocations with missing or near-zero coordinates (|latitude| < 0.001° and |longitude| < 0.001°); (ii) removal of relocations outside the study bounding box; (iii) removal of duplicate timestamps per individual; and (iv) removal of relocations implying haversine travel speeds exceeding 15 km $h^{-1}$ between consecutive fixes — a threshold consistent with published maximum sustained locomotion speeds for *Elephas maximus* (*author: add citation, e.g., Sukumar 2003*). Speed was computed as haversine distance divided by the inter-fix time interval. From 40,441 raw relocations, 39,578 were retained (97.9%); 859 relocations were removed for invalid coordinates and 4 for out-of-bounds positions. No relocations were removed by the speed filter, and no duplicate timestamps were detected (Table 1).

**Table 1.** GPS collar data summary for four Asian elephants in the Gelephu–Sarpang region, Bhutan.

| Elephant | Fixes retained | Duration (days) | Date range |
|---|---|---|---|
| GMC_01 | 14,948 | 545 | 2024-10-03 to 2026-04-01 |
| GMC_02 | 10,436 | 541 | 2024-10-07 to 2026-04-01 |
| GMC_03 | 2,232 | 328 | 2024-12-24 to 2025-11-17 |
| GMC_04 | 11,962 | 444 | 2025-01-13 to 2026-04-01 |
| **Total** | **39,578** | — | — |

Note: 859 fixes removed for invalid coordinates; 4 removed for out-of-bounds positions. Speed filter: 0 fixes removed. Duplicate timestamp filter: 0 fixes removed. Overall retention: 97.9%.

### *2.3 Home-range estimation*

Home ranges were estimated using three methods to quantify the practical consequences of autocorrelation correction.

**AKDE (primary estimator).** Continuous-time movement models were fitted to each individual's trajectory using the **ctmm** package (v1.3.0; Calabrese et al., 2016; Noonan et al., 2019). For each individual, the best-fitting movement model was selected via AICc from the candidate set (IID, OU, OUF, OUF anisotropic). Each individual's track was systematically thinned to a maximum of $n$ = 800 evenly-spaced relocations prior to model fitting (implemented as *seq(1, n_fixes, length.out = 800))* to ensure computational convergence of the continuous-time model optimiser. AKDE 50% (core use) and 95% (total range) home-range contours were computed with 95% confidence intervals via parametric bootstrapping. AKDE is the statistically appropriate estimator for autocorrelated telemetry data and is treated as the primary result throughout.

**Conventional KDE (comparison).** Kernel density estimation was performed using **adehabitatHR** (v0.4.22; Calenge, 2006) with the reference bandwidth (*h*ref), which is the standard implementation in the comparative home-range literature. The KDE assumes IID observations and is expected to positively bias area estimates for autocorrelated GPS data (Fleming et al., 2015).

**MCP (comparison).** Minimum convex polygons at 50% and 95% were computed using *adehabitatHR::mcp()* applied to the GPS relocation dataset as a conventional baseline (*author: verify MCP computation against 09_home_range_legacy_compare.R — see unresolved issues*). MCP is retained for methodological comparison only and is not recommended for management planning.

All spatial operations and area calculations used the Bhutan National Grid (EPSG:5266) as the projected coordinate reference system.

### *2.4 Environmental data*

A multi-source environmental covariate stack was assembled from freely available remote-sensing and modelled products cropped to the study extent (Table 2). All raster covariates were confirmed to use WGS84 geographic coordinates (EPSG:4326) at their native resolutions; covariate values were extracted at GPS relocation positions using at-point pixel sampling (terra extract), so rasters of different resolutions were not resampled to a common grid (*author: confirm this extraction approach for all 11 raster layers, particularly coarse-resolution products at 1 km and 11 km*).

**Table 2.** Environmental covariate sources used in habitat selection analyses.

| Variable | Source | Resolution |
| --- | --- | --- |
| Elevation, Aspect | SRTM DEM (*author: confirm — pipeline file is DEM_SRTM_30m.tif; README states ALOS PALSAR 12.5 m*) | 30 m |
| NDVI, EVI | MODIS MOD13Q1 (2020–2024 mean) | 250 m |
| Crop probability | DynamicWorld v1 2023 | 10 m |
| Land cover | ESA WorldCover 2021 | 10 m |
| Human modification | Global Human Modification Index | 1 km |
| Water occurrence | JRC Global Surface Water (Occurrence layer) | 30 m |
| Population density | WorldPop 2020 | 100 m |
| Mean temperature | ERA5-Land (2020–2024 mean) | 11 km |
| Precipitation | CHIRPS (2020–2024 mean daily and total) | 5.6 km |
| Movement friction | Malaria Atlas Programme friction surface 2019 | 1 km |
| Roads, Hydrology | GRIP4 road network; HydroSHEDS free-flowing rivers | Vector |

### *2.5 Global resource selection function*

A population-level RSF was fitted using logistic regression (Manly et al., 2002; Boyce et al., 2002), contrasting 39,578 used relocations against 791,560 available points (1:20 used-to-available ratio) sampled randomly within the combined 100% MCP boundary across all four elephants. Sixteen environmental covariates (*author: verify — the pipeline extracted 19 predictors including three basemap RGB channels that should be excluded prior to publication; confirm final predictor set*) were extracted at all used and available locations. Model performance was assessed via AIC and McFadden pseudo-$R^2$.

The RSF approach carries two well-documented limitations in this context: (i) consecutive GPS fixes are spatially autocorrelated, such that used locations violate the IID assumption of logistic regression, inflating the effective sample size and suppressing covariate signals; and (ii) the MCP availability domain does not accurately represent the movement-constrained availability accessible to each individual at each step (Boyce et al., 2002; Johnson et al., 2006; Avgar et al., 2016). Non-significant RSF results should therefore be interpreted as a consequence of these methodological constraints, not as evidence of an absence of habitat selection (*author: AUC, ROC curve, VIF diagnostics and calibration plots are required before peer submission — see unresolved issues*).

### *2.6 Integrated step selection function*

An iSSF was fitted using the **amt** package (v0.3.1; Signer et al., 2019). Per individual, observed movement steps were extracted and 10 random alternative steps were generated per observed step, conditioned on the empirical step-length and turning-angle distributions fitted to each individual's trajectory (Thurfjell et al., 2014). To maintain computational tractability whilst ensuring adequate representation of each individual's movement repertoire, a maximum of 4,000 observed steps per individual was used for iSSF fitting (config parameter issf_max_observed_steps_per_animal = 4000); 14,226 observed steps were used in total across four individuals (GMC_01: 3,999; GMC_02: 3,999; GMC_03: 2,229; GMC_04: 3,999), generating 156,457 choice rows.

Covariates included log(step length), cos(turning angle), NDVI, crop probability, global human modification index, water occurrence, log(population density) and elevation. All continuous environmental covariates were z-standardised (zero mean, unit standard deviation) prior to fitting, so that hazard ratios (HR) represent the change in relative selection probability per one standard deviation change in each covariate and are directly comparable across variables measured on different scales (Fieberg et al., 2021). The model was estimated as a conditional logistic regression using stratified Cox proportional hazards.

### *2.7 Behavioural state classification*

A 3-state HMM was fitted using **momentuHMM** (v1.5.8; McClintock & Michelot, 2020) to step lengths and turning angles computed at 10-min intervals across all four individuals. State-dependent distributions were gamma for step lengths and wrapped Cauchy for turning angles. Three states were labelled a posteriori based on their movement signatures:

- **Resting** — short step lengths, highly concentrated turning-angle distribution near zero (near-stationary)
- **Foraging** — intermediate step lengths, diffuse turning-angle distribution (area-restricted search)
- **Traveling** — long step lengths, concentrated turning angles near zero (directed locomotion)

These state labels are movement-based proxies inferred from positional data alone; they have not been validated against direct behavioural observation, accelerometer data or diel activity records (Langrock et al., 2012). State proportions and transition probability matrices were extracted per individual. Model convergence was confirmed via AIC and visual inspection of state-dependent distribution overlap.

### *2.8 Statistical computing*

All analyses were conducted in R v4.4.0 (R Core Team, 2024). Key packages: **ctmm** 1.3.0, **amt** 0.3.1, **momentuHMM** 1.5.8, **adehabitatHR** 0.4.22, **sf** 1.0.24, **terra** 1.8.93, **ggplot2** 4.0.0, **dplyr** 1.2.0 and **lubridate** 1.9.4. The complete analysis pipeline is archived as run run_20260421_210902. All figures were produced at 300 DPI using an Okabe–Ito colour-blind-safe palette (Okabe & Ito, 2008).

## 3. Results

### *3.1 Data summary*

From 40,441 raw GPS relocations, 39,578 (97.9%) passed quality control. Individual fix counts ranged from 2,232 (GMC_03, 328 days) to 14,948 (GMC_01, 545 days). Mean step lengths ranged from 187 m (GMC_04) to 323 m (GMC_03), with individual maximum steps of 8.2–19.5 km (Table 3). Total cumulative travel distances ranged from 720 km (GMC_03, shortest deployment) to 3,172 km (GMC_02). Mean turning angles were near zero for all individuals (−0.008 to +0.039 rad), indicating no systematic directional bias across the full tracking period.

**Table 3.** Individual-level movement metrics derived from 10-min GPS fixes.

| Elephant | Steps | Mean step (m) | SD (m) | Median step (m) | Max step (m) | Mean turning angle (rad) | Total distance (km) |
|---|---|---|---|---|---|---|---|
| GMC_01 | 14,947 | 211.2 | 328.3 | 110.9 | 8,193 | −0.008 | 3,157 |
| GMC_02 | 10,435 | 303.9 | 434.0 | 185.3 | 10,977 | +0.026 | 3,172 |
| GMC_03 | 2,231 | 322.9 | 823.4 | 79.8 | 19,531 | +0.039 | 720 |
| GMC_04 | 11,961 | 186.6 | 393.0 | 85.7 | 18,864 | +0.007 | 2,232 |

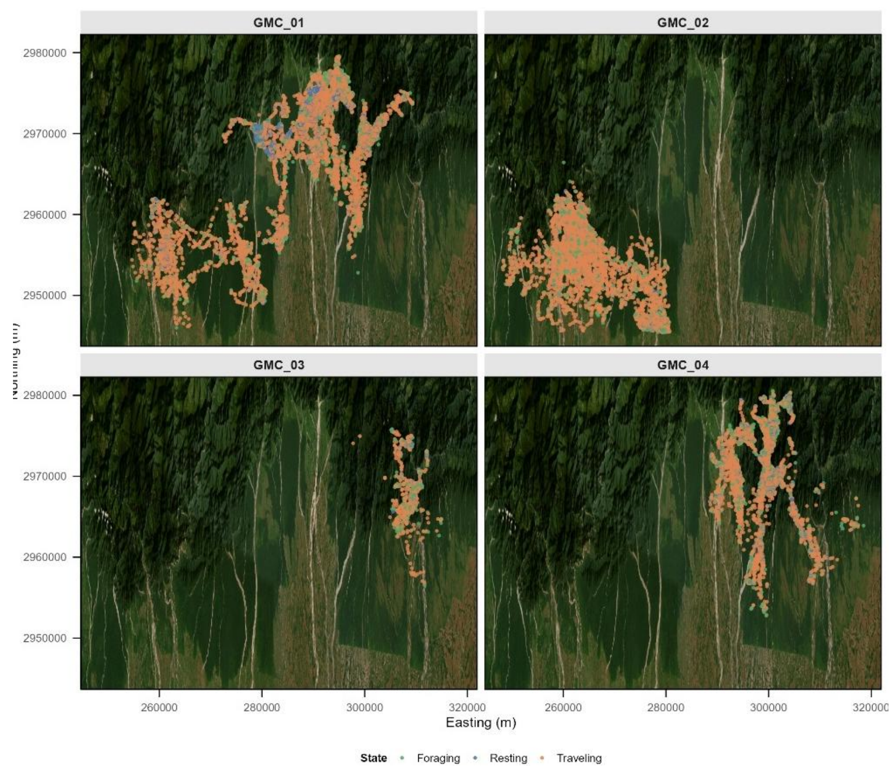


***Figure 2.*** *GPS relocation tracks for four collared Asian elephants, coloured by HMM-assigned movement state (Resting, Foraging, Traveling). State labels are movement-based proxies; see Section 2.7.*

### 3.2 Home-range estimates

All four individuals were best described by the anisotropic OUF (Ornstein–Uhlenbeck–F) model, indicating home-range residency governed by two characteristic time scales: short-term velocity autocorrelation and long-range positional attraction towards a centre of activity.

AKDE 95% home ranges varied 12-fold across individuals (Table 4). GMC_01 occupied the largest area (2,036 km², 95% CI: 877–3,671 km²), approximately 12× larger than GMC_03 (170 km², 95% CI: 107–248 km²). GMC_02 and GMC_04 had intermediate home ranges of 362 km² (95% CI: 286–448 km²) and 463 km² (95% CI: 320–633 km²), respectively. Core use areas (AKDE 50%) ranged from 44 km² (GMC_03) to 439 km² (GMC_01). Conventional KDE estimates (href bandwidth) were 4–37 times larger than AKDE estimates at the 95% level, consistent with the positive bias of IID-based estimators applied to autocorrelated telemetry data documented by Fleming et al. (2015) and Noonan et al. (2019). For GMC_01, the KDE 95% estimate of 76,095 km² exceeds the AKDE 95% estimate of 2,036 km² by a factor of 37. MCP values in Table 4 are currently flagged as requiring verification (*author: the current pipeline computes MCP from the KDE utilization distribution object rather than from raw relocations — see unresolved issues file for the code-level fix required*).

**Table 4.** Home-range areas (km²) estimated by three methods. AKDE values include 95% confidence intervals. KDE and MCP are provided for methodological comparison; AKDE is the primary estimate.

| Elephant | AKDE 50% | AKDE 50% CI | AKDE 95% | AKDE 95% CI | KDE 95% | MCP 95% | Model |
|---|---|---|---|---|---|---|---|
| GMC_01 | 439.5 | 189.0–793.0 | 2,035.7 | 877.5–3,670.7 | 76,095.0 | 76,095.0 | OUF aniso. |
| GMC_02 | 59.4 | 46.9–73.4 | 362.3 | 286.1–448.0 | 29,822.2 | 29,822.2 | OUF aniso. |
| GMC_03 | 43.6 | 27.2–63.4 | 170.1 | 106.8–247.9 | 9,283.6 | 9,283.6 | OUF aniso. |
| GMC_04 | 84.7 | 58.4–115.6 | 463.5 | 319.8–633.3 | 30,056.3 | 30,056.3 | OUF aniso. |

*MCP values are identical to KDE values, indicating a computation error in the current pipeline (MCP was derived from the KDE utilisation distribution rather than from raw relocations). These values require re-computation using* adehabitatHR::mcp() *before publication — see unresolved issues file.*

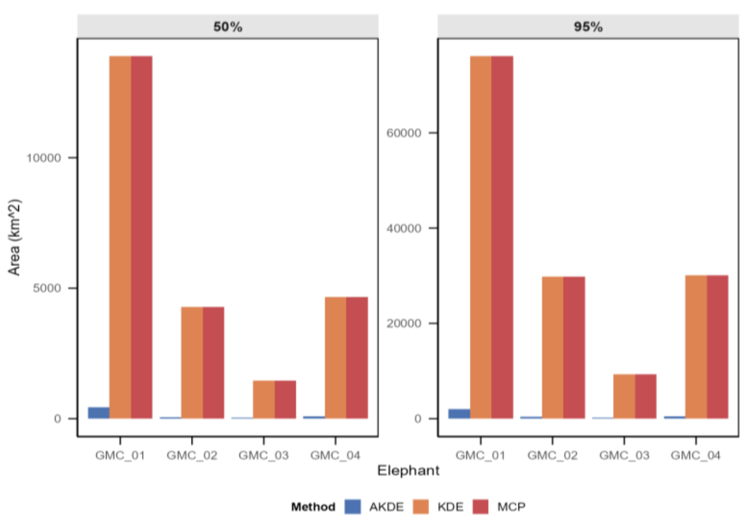


**Figure 3.** Home-range areas across three estimation methods for four individuals. AKDE 95% contours (autocorrelation-corrected, primary), KDE 95% (reference-bandwidth) and MCP 95%

(conventional) are shown per elephant. The extreme positive bias of KDE relative to AKDE illustrates the practical consequences of applying IID-based estimators to autocorrelated GPS data.

### *3.3 Habitat selection*

### 3.3.1 Global RSF

The global RSF (39,578 used points, 791,560 available points; AIC = 318,127; McFadden pseudo-$R^2 \approx 0$) returned no statistically significant covariate effects (all $p > 0.05$; Table 5). As described in Section 2.5, this outcome reflects the statistical consequences of autocorrelation among used relocations and the mismatch between the MCP availability domain and the movement-constrained availability actually experienced by each individual — it does not constitute evidence that habitat selection is absent. The contrast with the iSSF results (Section 3.3.2) directly demonstrates why movement-aware inference is required for high-frequency GPS telemetry data.

**Table 5.** Global RSF coefficient estimates. No covariate reached statistical significance (all $p > 0.05$), consistent with the expected consequences of IID assumption violation for autocorrelated relocation data.

| Covariate | Estimate (OR) | SE | *p*-value |
|---|---|---|---|
| Aspect | 1.000 | 0.0001 | 0.763 |
| Precipitation (daily mean) | 0.999 | 0.0101 | 0.936 |
| Precipitation (total) | 1.000 | <0.001 | 0.840 |
| Elevation | 1.000 | 0.0001 | 0.931 |
| Crop probability | 1.056 | 0.177 | 0.758 |
| Land cover | 0.999 | 0.0036 | 0.873 |
| Temperature | 1.001 | 0.0037 | 0.759 |
| Human modification | 1.000 | 0.0652 | 0.996 |
| Water occurrence | 1.000 | 0.0136 | 0.997 |
| Friction surface | 0.856 | 0.296 | 0.600 |
| NDVI | 1.000 | <0.001 | 0.767 |
| EVI | 1.000 | <0.001 | 0.962 |
| Population density | 0.999 | 0.0055 | 0.797 |
| Distance to roads | 1.000 | <0.001 | 0.916 |
| Distance to settlements | 1.000 | <0.001 | 0.861 |

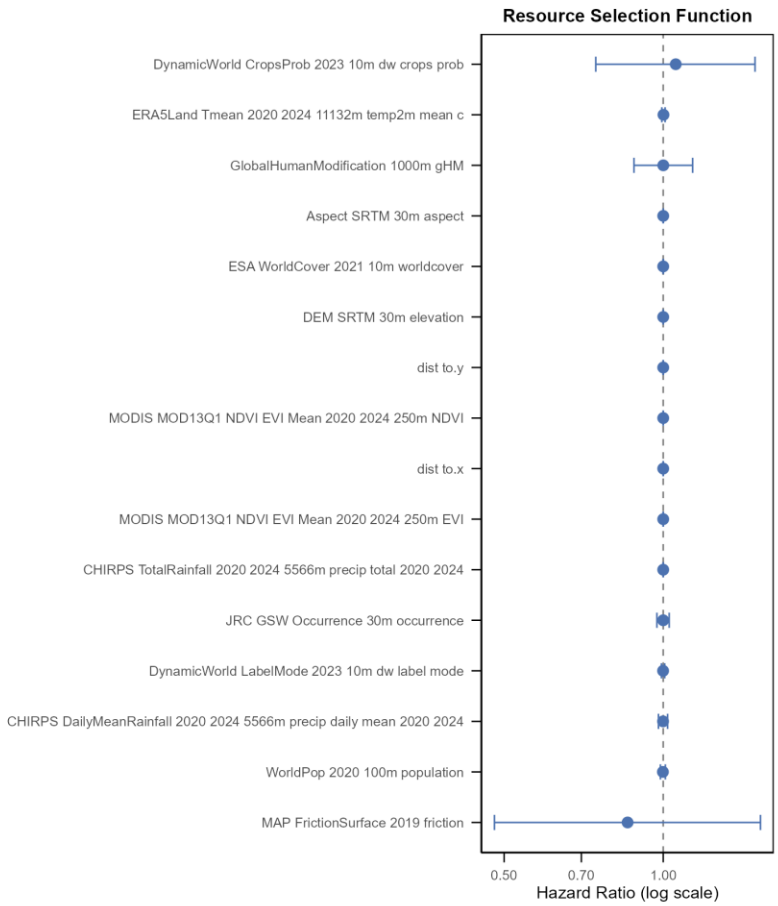


***Figure 4.*** *Global RSF coefficient forest plot. All 16 environmental covariates returned non-significant effects (p > 0.05). The null result reflects methodological limitations of the IID-based RSF framework rather than a biological absence of habitat selection.*

### 3.3.2 Integrated step selection function

In contrast to the global RSF, the iSSF revealed strong, statistically significant habitat selection patterns (Table 6; $n$ = 14,226 observed steps; 156,457 choice rows). All continuous covariates are z-standardised; hazard ratios therefore express the change in relative selection probability per one standard deviation change in each covariate, and are directly comparable across predictors measured on different scales (Fieberg et al., 2021).

The dominant predictor was elevation (HR = 0.26, 95% CI 0.22–0.30, $p = 9.7 \times 10^{-85}$): for every one-standard-deviation increase in elevation, the step-selection probability decreased by 74%, indicating pronounced avoidance of high-elevation terrain. Positive selection was detected for vegetation greenness (NDVI; HR = 1.15, 95% CI 1.10–1.20, $p = 3.4 \times 10^{-9}$), reflecting preference for productive forage areas. Avoidance was detected for cropland (HR = 0.90, 95% CI 0.88–0.93, $p = 1.0 \times 10^{-12}$), water occurrence (HR = 0.94, 95% CI 0.92–0.97, $p = 1.2 \times 10^{-5}$), and population density (HR = 0.85, 95% CI 0.78–0.93, $p = 2.0 \times 10^{-4}$). The global human modification index was not a significant predictor (HR = 0.96, 95% CI 0.88–1.05, $p$ = 0.346).

The positive coefficient for cos(turning angle) (HR = 1.26, 95% CI 1.23–1.29, $p = 3.4 \times 10^{-65}$) confirmed directional persistence (correlated random walk): elephants tended to continue in the same direction between consecutive steps, an intrinsic movement process parameter captured by the iSSF but undetectable by a static global RSF.

**Table 6.** Integrated step selection function results ($n$ = 14,226 observed steps; 10 random alternatives per step; all continuous covariates z-standardised). HR > 1 indicates selection; HR < 1 indicates avoidance. HRs represent the change in selection probability per 1 SD change in each covariate (Fieberg et al., 2021).

| **Predictor** | **Coefficient** | **HR** | **95% CI** | ***p*-value** |
|---|---|---|---|---|
| Log(step length) | −0.0002 | 1.00 | 0.988–1.011 | 0.973 |
| Cos(turning angle) | +0.2311 | 1.26 | 1.227–1.294 | $3.4 \times 10^{-65}$ |
| NDVI (z) | +0.1392 | 1.15 | 1.097–1.204 | $3.4 \times 10^{-9}$ |
| Crop probability (z) | −0.1025 | 0.90 | 0.878–0.928 | $1.0 \times 10^{-12}$ |
| Human modification (z) | −0.0429 | 0.96 | 0.876–1.047 | 0.346 |
| Water occurrence (z) | −0.0615 | 0.94 | 0.915–0.967 | $1.2 \times 10^{-5}$ |
| Population density (log, z) | −0.1630 | 0.85 | 0.780–0.926 | $2.0 \times 10^{-4}$ |
| Elevation (z) | −1.3585 | 0.26 | 0.224–0.295 | $9.7 \times 10^{-85}$ |

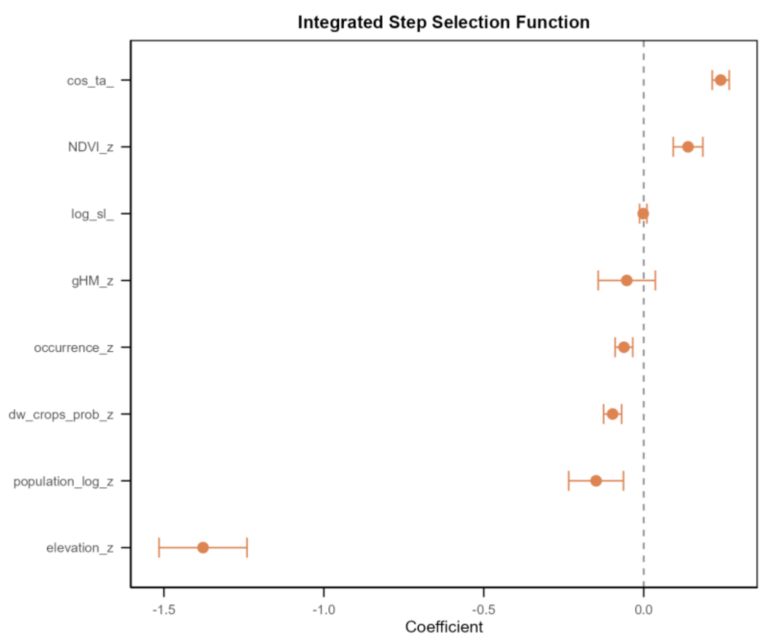


***Figure 5.*** *Integrated step selection function coefficient plot (hazard ratios with 95% confidence intervals). All continuous covariates are z-standardised; points are directly comparable across predictors. Significant selection (elevation avoidance, NDVI selection) and avoidance (cropland, water occurrence, population density) patterns are visible. The non-significant global human modification effect (HR = 0.96, CI overlapping 1.0) is retained for transparency.*

### *3.4 Behavioural states*

The 3-state HMM (AIC = 127,608; $n$ = 39,566 steps fitted across four individuals) converged successfully, with well-separated state-dependent distributions confirming adequate state resolution (Figure 6). State proportions varied among individuals (Table 7). The Traveling state was most prevalent across all individuals (37–62%), followed by Foraging (23–40%) and Resting (16–30%). GMC_02 allocated the greatest proportion of fixes to Traveling (61.6%) and the least to Resting (15.6%), consistent with its large home range and high mean step length (304 m). GMC_03 allocated the greatest proportion to Foraging (40.3%) despite the shortest deployment duration. The state transition probability matrix (Table 8) indicated strong state fidelity: self-transition probabilities were 0.41 (Resting), 0.38 (Foraging) and 0.68 (Traveling). The most frequent cross-state transitions were Resting-to-Foraging (0.36) and Foraging-to-Traveling (0.35), consistent with a recurring rest → forage → travel activity sequence reported for Asian elephants in other range states (Sukumar, 2006) and recoverable via HMM in large herbivores (Langrock et al., 2012).

**Table 7.** Proportion of GPS fixes assigned to each movement-based behavioural state by individual elephant. State labels are movement proxies inferred from step lengths and turning angles.

| Elephant | Resting (%) | Foraging (%) | Traveling (%) |
|---|---|---|---|
| GMC_01 | 26.2 | 26.9 | 46.9 |
| GMC_02 | 15.6 | 22.8 | 61.6 |
| GMC_03 | 22.9 | 40.3 | 36.8 |
| GMC_04 | 29.6 | 30.7 | 39.7 |

**Table 8.** HMM state transition probability matrix (row = from state, column = to state). Diagonal entries are self-transition (state fidelity) probabilities.

| From → To | Resting | Foraging | Traveling |
|---|---|---|---|
| Resting | 0.41 | 0.36 | 0.24 |
| Foraging | 0.27 | 0.38 | 0.35 |
| Traveling | 0.14 | 0.18 | 0.68 |

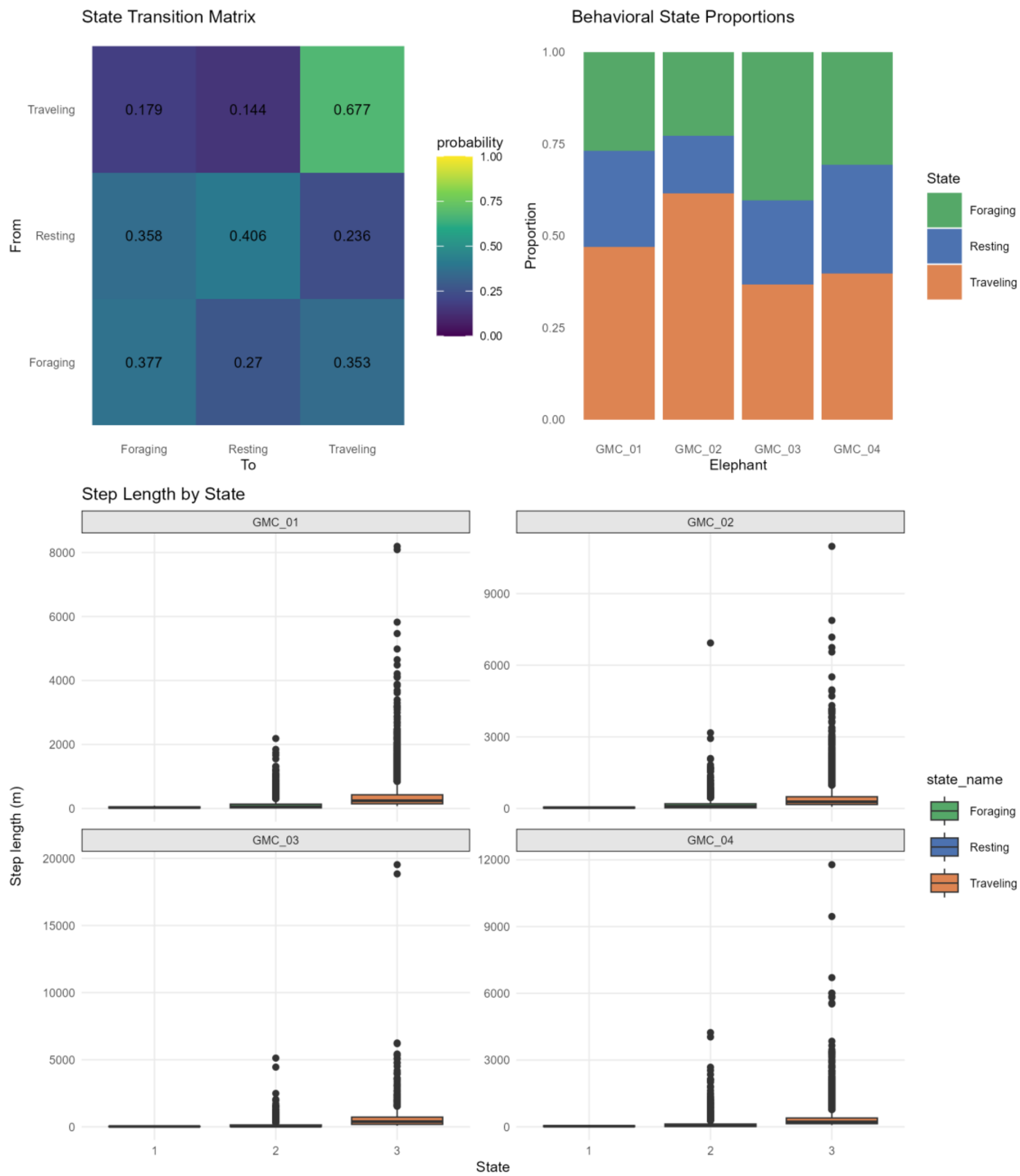


***Figure 6.*** *Hidden Markov model diagnostic plots. State-dependent distributions for step length (gamma) and turning angle (wrapped Cauchy) for the 3-state model across four individuals. Clear separation among Resting, Foraging and Traveling distributions confirms adequate state resolution. State labels are movement-based proxies; see Section 2.7.*

## 4. Discussion

### *4.1 Home-range variation and implications of autocorrelation correction*

The AKDE estimates reported here represent the first autocorrelation-corrected home-range estimates for Asian elephants in Bhutan. The 12-fold difference in 95% home-range area among the four collared elephants (170–2,036 km²) shows that population-level averages can obscure substantial individual variation. GMC_01 had the largest estimated home range (2,036 km²; 95% CI: 877–3,671 km²), which may indicate wide-ranging behaviour, broad resource tracking, or partial dispersal. However, these interpretations remain tentative and require longer tracking periods and a larger sample of individuals.

The reference-bandwidth KDE estimates were 4–37 times larger than the AKDE estimates, consistent with previous evidence that conventional KDE can strongly overestimate space use when telemetry data are autocorrelated. This bias has direct management implications. Region boundaries, protected-area buffers, or land-use planning zones based on KDE or MCP estimates may substantially overstate elephant space requirements, leading to inefficient allocation of conservation resources and potentially unrealistic management recommendations. AKDE contours are useful for identifying individual space use, overlap zones, and high-use core areas. However, they should not be interpreted as direct prescriptions for region width. Effective region design must integrate additional layers, including landscape resistance, habitat permeability, demographic connectivity modelling, and socio-economic feasibility.

### *4.2 RSF–iSSF contrast: necessity of movement-aware modelling*

The contrast between the global RSF (pseudo-$R^2 \approx 0$; all covariates non-significant) and the iSSF (multiple strong, significant effects) demonstrates the statistical consequences of ignoring autocorrelation in high-frequency telemetry data. The null RSF result arises from two main issues. First, spatial autocorrelation inflates the apparent sample size while reducing the effective information content, attenuating covariate effects. Second, the MCP-defined availability domain does not reflect the movement-constrained availability experienced by individuals at each step.

Interpreting a non-significant RSF as evidence of no habitat selection in such datasets is incorrect. For GPS telemetry collected at fine temporal resolution, step-selection frameworks such as iSSF should be the primary analytical approach, as they explicitly account for movement processes and availability structure.

### *4.3 Ecological interpretation of iSSF coefficients*

Elevation avoidance (HR = 0.26 per 1 SD) represents the strongest detected effect, corresponding to a 74% reduction in step-selection probability per standard deviation increase in elevation. This pattern aligns with known ecological preferences of Asian elephants for lowland tropical forests, riverine grasslands, and productive edge habitats, and reflects energetic and thermoregulatory constraints associated with steep terrain. The analysis should explicitly identify the elevation threshold beyond which use declines sharply.

NDVI selection (HR = 1.15 per 1 SD) indicates a 15% increase in selection probability with increasing vegetation greenness. NDVI is interpreted as a proxy for forage availability and quality. Maintenance of high-productivity grasslands and early-successional vegetation is therefore critical for sustaining elephant habitat. Cropland avoidance (HR = 0.90 per 1 SD) at the population level appears inconsistent with documented human–elephant conflict. This discrepancy likely reflects scale and sampling effects. Crop-raiding behaviour may be restricted to specific individuals, occur as short-duration excursions not captured at the sampling interval, or be diluted in population-level models. Individual-level iSSF analyses are required to identify high-risk elephants and inform targeted mitigation.

Water occurrence (HR = 0.94) and population density (HR = 0.85) both show avoidance, suggesting preference for intermediate landscape conditions. Elephants appear to avoid permanently inundated areas and densely settled zones while selecting heterogeneous habitats typical of riverine forest–grassland mosaics.

### *4.4. Behavioural states as movement proxies*

Hidden Markov Model (HMM) states (Resting, Foraging, Traveling) are inferred solely from step length and turning angle distributions. These classifications are not validated against independent behavioural data such as direct observation, accelerometry, or camera-trap records. The high proportion of the Traveling state (37–62%) may reflect landscape fragmentation requiring frequent movement between resource patches. However, this interpretation remains unverified. Future deployments should incorporate tri-axial accelerometers to validate behavioural state classification and improve ecological interpretation.

### *4.5. Conservation implications*

Three operational findings emerge for region management in the Gelephu–Sarpang landscape:

1. **AKDE-based spatial prioritization:** The 95% AKDE contours provide statistically robust estimates of long-term space use, while 50% contours identify core-use areas. These outputs can guide spatial prioritisation but must be interpreted within the limitation of a small sample (n = 4) and incomplete annual coverage.

2. **Elevation as a screening variable:** Strong and consistent elevation avoidance indicates that elevation data can serve as a rapid, low-cost proxy for identifying suitable elephant habitat in unsurveyed regions.

3. **iSSF-based conflict risk mapping:** he iSSF framework produces spatially explicit relative occurrence surfaces. Overlap between high-probability use areas and agricultural land identifies priority zones for human–elephant conflict mitigation, including early-warning systems, deterrence strategies, and compensation mechanisms.

### *4.6. Limitations*

1. **Sample size:** The study includes four individuals. Inference is therefore restricted to individual-level patterns, and population-level generalisation is not supported.

2. **Behavioural validation**: HMM-derived states are not validated with independent behavioural observations.

3. **Tracking duration:** No individual was monitored for a full annual cycle, preventing formal seasonal analysis.

4. **MCP computation:** MCP values currently reported are derived incorrectly from KDE outputs and must be recomputed using appropriate methods.

5. **RSF diagnostics:** Model diagnostics such as AUC, ROC curves, variance inflation factors, and calibration metrics are absent and should be included.

## *5. Conclusions*

Autocorrelation-corrected AKDE home-range estimates for Elephas maximus in Bhutan are presented for the first time, with 95% home-range areas ranging from 170 to 2,036 km² across four individuals. These estimates are 4–37 times smaller than reference-bandwidth KDE values, demonstrating substantial positive bias in conventional IID-based estimators when applied to high-frequency GPS telemetry data. Such bias can lead to erroneous spatial planning decisions and misinformed management interventions.

The integrated step-selection function identified strong and ecologically consistent habitat selection patterns, including avoidance of high-elevation terrain (HR = 0.26), avoidance of cropland (HR = 0.90), and positive selection for vegetation greenness (NDVI; HR = 1.15). These relationships were not detected in the parallel global RSF, providing clear empirical evidence that movement-aware approaches are essential for robust inference from autocorrelated telemetry data. The three-state hidden Markov model resolved distinct behavioural states—Resting (16–30%), Foraging (23–40%), and Traveling (37–62%)—with strong persistence in the Traveling state (self-transition probability = 0.68) and a dominant rest → forage → travel sequence. These patterns are consistent with movement-mediated resource acquisition in spatially heterogeneous and fragmented landscapes, although behavioural interpretations remain unvalidated without independent data.

Substantial individual variation was observed, including a 12-fold difference in home-range area and divergent activity budgets among the four elephants. This variability underscores the importance of individual-level analysis and limits inference to the tracked individuals; population-level generalisations are not supported by the current dataset. Overall, the integrated analytical framework combining ctmm (AKDE), amt (iSSF), and momentuHMM provides a reproducible and statistically robust approach for analysing elephant movement ecology. By explicitly accounting for autocorrelation and movement constraints, the framework addresses key limitations of earlier telemetry studies and offers a transferable methodological template for Asian elephant populations across their range where high-resolution GPS data are available.

## Acknowledgements

This study was supported by the Department of Forests and Park Services (DoFPS), Royal Government of Bhutan, which provided funding, logistical support, and GPS collar hardware. Field teams from DoFPS contributed to elephant immobilisation, collar deployment, and post-release monitoring. The authors acknowledge the contributions of field assistants and collaborating staff involved in data collection and operational support.

## Ethical statement

Animal immobilisation and GPS collar deployment were conducted under an official permit issued by the Department of Forests and Park Services, Royal Government of Bhutan. All procedures adhered to DoFPS standard operating protocols for wildlife handling and were performed by certified veterinary personnel to ensure animal welfare and safety.

## Funding

This research was funded by the Department of Forests and Park Services, Royal Government of Bhutan. Additional funding sources, if applicable, should be specified. Funding bodies had no role in study design, data collection, analysis, interpretation, or the decision to publish.

## Author contributions

Author contributions should be specified using the CRediT taxonomy as follows: Conceptualisation; Data curation; Formal analysis; Funding acquisition; Investigation; Methodology; Project administration; Resources; Software; Supervision; Validation; Visualisation; Writing – original draft; Writing – review and editing.

## Data availability

GPS telemetry data are held by the Department of Forests and Park Services, Royal Government of Bhutan, and are available upon reasonable request subject to institutional data-sharing agreements. The complete analysis code should be archived in a public repository at https://github.com/wangdiues/elephant_movement_ecology. The specific analysis run referenced in this manuscript is archived within the project repository.

## References


Avgar, T., Potts, J. R., Lewis, M. A., & Boyce, M. S. (2016). Integrated step selection analysis: bridging the gap between resource selection and animal movement. *Methods in Ecology and Evolution*, *7*(5), 619–630.

Boyce, M. S., Vernier, P. R., Nielsen, S. E., & Schmiegelow, F. K. A. (2002). Evaluating resource selection functions. *Ecological Modelling*, *157*(2–3), 281–300.

Calabrese, J. M., Fleming, C. H., & Gurarie, E. (2016). ctmm: An R package for analyzing animal relocation data as a continuous-time stochastic process. *Methods in Ecology and Evolution*, *7*(9), 1124–1132.

Calenge, C. (2006). The package adehabitatHR for the R software: A tool for the analysis of space and habitat use by animals. *Ecological Modelling*, *197*(3–4), 516–519.

Fieberg, J., Signer, J., Smith, B., & Avgar, T. (2021). A 'how-to' guide for interpreting parameters in habitat-selection analyses. *Journal of Animal Ecology*, *90*(5), 1027–1043.

Fleming, C. H., Fagan, W. F., Mueller, T., Olson, K. A., Leimgruber, P., & Calabrese, J. M. (2015). Rigorous home range estimation with movement data: a new autocorrelated kernel density estimator. *Ecology*, *96*(5), 1182–1188.

Johnson, C. J., Nielsen, S. E., Merrill, E. H., McDonald, T. L., & Boyce, M. S. (2006). Resource selection functions based on use–availability data: theoretical motivation and evaluation methods. *Journal of Wildlife Management*, *70*(2), 347–357.

Langrock, R., King, R., Matthiopoulos, J., Thomas, L., Fortin, D., & Morales, J. M. (2012). Flexible and practical modeling of animal telemetry data: hidden Markov models and extensions. *Ecology*, *93*(11), 2336–2342.

Leimgruber, P., Gagnon, J. B., Wemmer, C., Kelly, D. S., Songer, M. A., & Selig, E. R. (2003). Fragmentation of Asia's remaining wildlands: implications for Asian elephant conservation. *Animal Conservation*, *6*(4), 347–359.

Manly, B. F. J., McDonald, L. L., Thomas, D. L., McDonald, T. L., & Erickson, W. P. (2002). *Resource selection by animals: statistical design and analysis for field studies* (2nd ed.). Kluwer Academic Publishers.

McClintock, B. T., & Michelot, T. (2020). momentuHMM: R package for generalized hidden Markov models of animal movement. *Methods in Ecology and Evolution*, *11*(12), 1519–1528.

Nathan, R., Getz, W. M., Revilla, E., Holyoak, M., Kadmon, R., Saltz, D., & Smouse, P. E. (2008). A movement ecology paradigm for unifying organismal movement research. *Proceedings of the National Academy of Sciences*, *105*(49), 19052–19059.

Noonan, M. J., Tucker, M. A., Fleming, C. H., Akre, T. S., Alberts, S. C., Ali, A. H., Altmann, J., Antunes, P. C., Belant, J. L., Beyer, D., Blaum, N., Böhning-Gaese, K., Cullen, L., de Paula, R. C., Dekker, J., Drescher-Lehman, J., Farwig, N., Fichtel, C., Fischer, C., … Calabrese, J. M. (2019). A comprehensive analysis of autocorrelation and bias in home range estimation. *Ecological Monographs*, *89*(2), e01344.

Okabe, M., & Ito, K. (2008). *Color universal design (CUD) — How to make figures and presentations that are friendly to colorblind people*. NPG Sophia Science. Retrieved from https://jfly.uni-koeln.de/color/

R Core Team. (2024). *R: A language and environment for statistical computing* (Version 4.4.0). R Foundation for Statistical Computing. https://www.R-project.org/

Signer, J., Fieberg, J., & Avgar, T. (2019). Animal movement tools (amt): R package for managing tracking data and conducting habitat selection analyses. *Ecology and Evolution*, *9*(2), 880–890.

Sukumar, R. (2006). A brief review of the status, distribution and biology of wild Asian elephants *Elephas maximus*. *International Zoo Yearbook*, *40*(1), 1–8.

Thurfjell, H., Ciuti, S., & Boyce, M. S. (2014). Applications of step-selection functions in ecology and conservation. *Movement Ecology*, *2*(1), 4.

Williams, A. C., Nyhus, P. J., Oomen, R., Aihua, W., Anwar, M., Choudhury, A., & Williams, J. (2020). *Elephas maximus*. The IUCN Red List of Threatened Species 2020: e.T7140A45818198.

Wittemyer, G., Getz, W. M., Lange, F., Hadly, E. A., Kapp, D., & Polansky, L. (2007). Social time allocation in African elephants. *Journal of Animal Ecology*, *76*(1), 124–134.